Brillouin Spectroscopy

Subjects: Biochemistry & Molecular Biology

Contributor: María Victoria Gómez-Gaviro

Brillouin spectroscopy has recently gained considerable interest within the biomedical field as an innovative tool to study mechanical properties in biology. The Brillouin effect is based on the inelastic scattering of photons caused by their interaction with thermodynamically driven acoustic modes or phonons and it is highly dependent on the material's elasticity. Therefore, Brillouin is a contactless, label-free optic approach to elastic and viscoelastic analysis that has enabled unprecedented analysis of ex vivo and in vivo mechanical behavior of several tissues with a micrometric resolution, paving the way to a promising future in clinical diagnosis.

Brillouin spectroscopy diagnosis mechanics viscoelasticity biological tissues

1. Introduction

As the role of mechanical properties of cells and tissues is gaining high relevance in the study of a wide range of biological processes, Brillouin imaging has emerged as a promising tool for the characterization of biological samples in terms of their viscoelastic behavior. Traditional techniques for the characterization of biomaterials such as magnetic bead twisting, deformation microscopy, micro-rheology, or atomic force microscopy (AFM) either require contact, are destructive, or do not provide sufficient resolution. Conventional optical coherence elastography, which is a clinical tool that measures tissue biomechanics, is very sensitive to environmental vibrations [1]. On the contrary, Brillouin imaging presents a contactless, label-free, non-destructive modality for probing biological samples in the GHz/micron scale and with great potential in clinical diagnosis.

The Brillouin light scattering (BS) effect was predicted by Léon Brillouin [2][3] and Leonid I. Mandelstam [4][5][6] independently in 1922 and 1926, respectively. However, there is controversy due to the possibility that L. I. Mandelstam had already presented this effect in 1918 [7]. L. I. Mandelstam joined Eugenii Gross to detect the BS experimentally, becoming the first person to observe the Brillouin effect and offer empirical confirmation [8].

The laser's invention in the 1960s brought a light source powerful enough to reduce acquisition times and increase the resolution, resulting in hundreds of experimental works in the area of condensed matter and becoming a consolidated tool [8][9]. Following the theoretical model presented by L. Brillouin and L. I. Mandelstam, Brillouin–Mandelstam scattering (for the sake of simplicity, it will be only denoted as Brillouin scattering (BS)) is based on the light's interaction with collective fluctuations of density in the physical medium, provoking a change in the frequency of the scattered light; this effect is explained by a sort of Doppler effect in addition to the Bragg condition to obtain constructive interference.

The first examples of BS measurements on biological tissues were described in the late 1970s and early 1980s that demonstrated the power of this system as a research tool of high resolution and sensitivity [10][11]. Following the development of the virtually imaged phased array (VIPA) spectrometers in 1996 and the introduction of Brillouin imaging in 2005, the topic has flourished into a prolific and fast-moving research field [12][13][14]. During the last decade, a great variety of applications of BS to biology and biomedicine has been reported. BS has been tested as a screening and diagnostic tool and a monitoring resource for a wide range of biological samples at cellular and tissue resolution [15]. This work aims to offer an overview of the development of BS-based techniques in biology, offering a comprehensive summary of the currently available literature and state-of-the-art instrumentation, and explores possible future outlooks (**Figure 1**A,B).

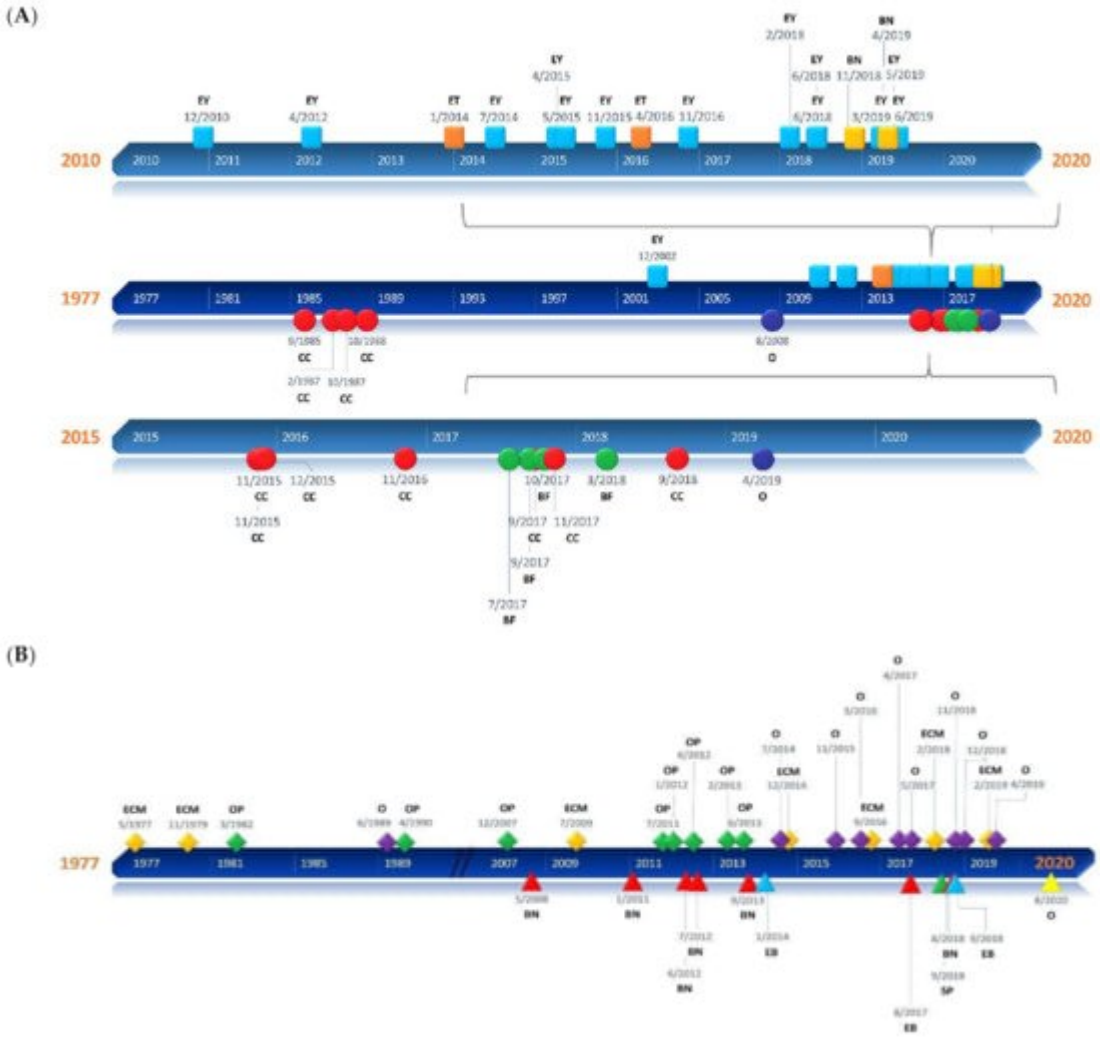

Figure 1. Timelines of the different applications presented in the review. (**A**) Square milestones represent publications related to human applications of Brillouin and have been classified into three groups: ophthalmology (EY), epithelial tissue (ET), and bone (BN). Circular milestones represent publications related to Brillouin microscopic studies regarding subcellular components (CC), biofilms (BF), and others (O). (**B**) Rhomboidal milestones represent Brillouin studies of animal tissues such as extracellular matrix (ECM), ephthalmological tissues (OP) such as the cornea or crystalline lenses, and others (O) that include neuronal, vascular, and

oncological applications, among others. Triangular milestones represent publications related to Brillouin studies of animal organs such as bone (BN), spine (SP), embryos (EB), or others (O).

2. Brillouin Light Scattering

2.1. Physical Basis

Scattering of light results from the interaction of the electromagnetic field with the constituents of the physical medium. That is the reason why a laser beam can be seen in directions other than the propagation direction. The scattered light can be more or less intense depending on the density of the physical medium and the particle size. The scattered light is composed of different components: one component corresponds to the original frequency (Rayleigh) and others result from intense frequency changes (Raman) or very subtle ones (Brillouin). Apart from the energy change in the scattered light, another relevant difference between Raman and Brillouin scattering includes the physical origin of the effect. In a simplified manner, the intramolecular vibrations are relevant in Raman scattering and the low energy collective vibrations are relevant for Brillouin scattering. The magnitude of the Brillouin-scattered light is about 10^3 times smaller than the Raman component and its frequency changes only about 10^{-6}–10^{-5} times with respect to the incident laser light; therefore, it is very challenging to assess.

The classical explanation of the Brillouin effect relies on the interaction of the electric field of the light with thermal fluctuations of the dielectric constant of the physical medium as first described in 1880 by the Lorentz–Lorenz equation. A historical review of this formula is presented by H. Kragh [16]:

$$\frac{n^2-1}{n^2+2} = r\,\rho \qquad (1)$$

where $n^2 = \varepsilon$; n is the refractive index and ε is the dielectric constant, r is the specific refractivity, and ρ the mass density.

However, a new vision of the Brillouin–Mandelsatm effect arises with the introduction of quantum mechanical approaches. Light is constituted by photons that behave as if they suffer an inelastic collision when traversing a physical medium (**Figure 2**A). The counterpart of this collision is the collective vibrations of the medium. These vibrations can be expressed in eigenmodes and can thus be treated as quasiparticles (phonons). In an inelastic collision, energy and momentum must be conserved, resulting in the following relationships:

$$\begin{aligned} \boldsymbol{k}^s - \boldsymbol{k}^i &= \pm\boldsymbol{q} \text{ (momentum conservation)} \\ \omega^s - \omega^i &= \pm\omega(\boldsymbol{q}) \text{ (energy conservation)} \end{aligned} \qquad (2)$$

where $\boldsymbol{k}^s$ and $\boldsymbol{k}^i$ correspond to the scattered and incident light wave vectors, $\boldsymbol{q}$ is the acoustic wave vector, ω^s and ω^i correspond to the scattered and incident light's physical frequencies, and $\omega(\boldsymbol{q})$ is the acoustic frequency. The

shift in the probing light's frequency is therefore equivalent to the acoustic frequency of the phonons and it is known as the Brillouin shift. Hard media have high acoustic frequencies and therefore larger Brillouin shifts than soft media. The Brillouin shift is also highly dependent on the temperature of the media as thermal energy increases the vibrational frequency of phonons (**Figure 2**B).

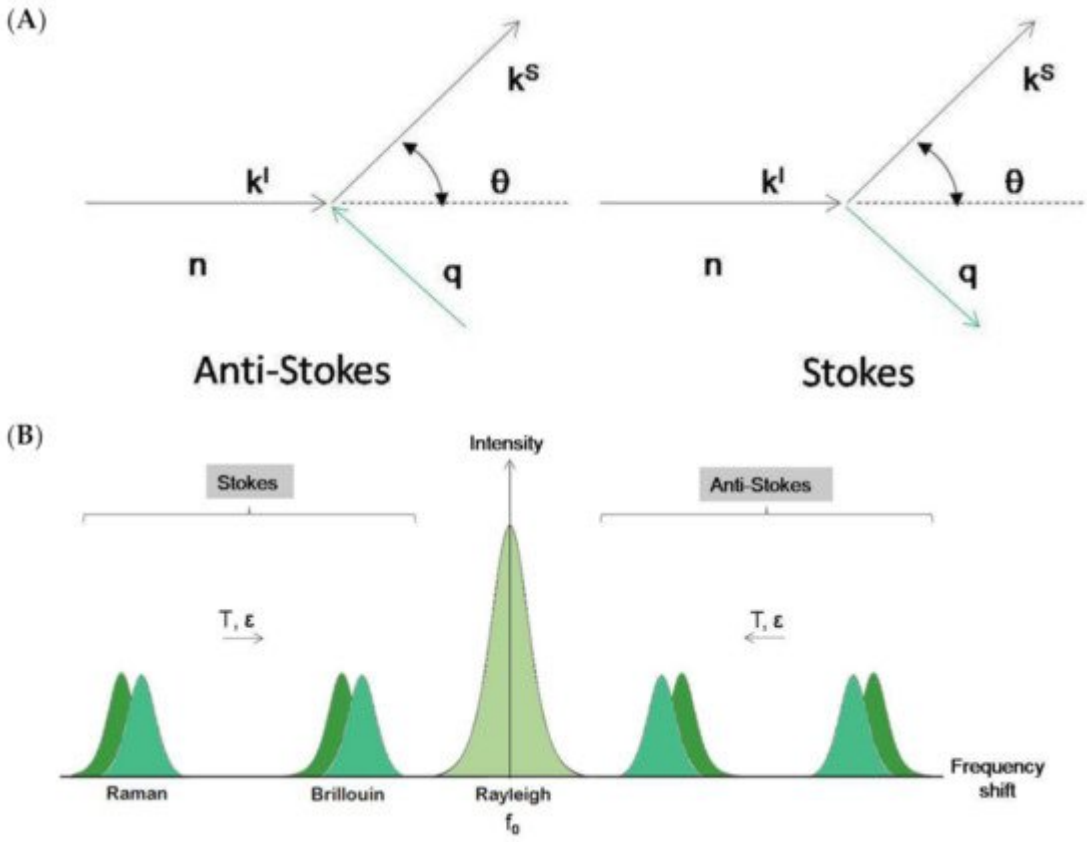

Figure 2. (**A**). Schematic representation of the Brillouin–Mandelstam effect as a collision between photon (***k****I*) and phonon (***q***). n is the refractive index of the physical medium and *θ* is the scattering angle. (**B**). Schematic representation of Brillouin and Raman spectra. In both experimental techniques, a small amount of light undergoes inelastic scatter, gaining or losing energy and giving rise to a couple of symmetric, frequency-shifted peaks in the spectrum. The remaining elastically scattered light (Rayleigh scatter) appears as a broad central peak with the same frequency as the incident light (f_0). In Brillouin and Raman spectroscopies, peak frequency position varies with temperature (*T*) and strain (*ε*). In Raman spectroscopy, the intensity ratio between Stokes and anti-Stokes peaks varies also with *T*.

This picture, which may be mathematically but not conceptually simple (**Figure 2**A), is well established in solid state physics and is based on a crystalline lattice. In systems without crystalline lattice, as is the case of liquids or glasses, the concept of hydrodynamic modes has been successfully introduced [17][18]. A typical Brillouin scattering spectrum is shown in **Figure 2**B.

The stimulated Brillouin spectroscopy (SBS) is a conceptually different method that has been recovered and is being considered for biomedical research. This method has shown its potential in liquids and some polymers [19],

and is based on the interference of two incident laser beams traversing the sample in different directions but crossing in a defined sample region. A density diffraction grid is stimulated (mainly by electrostriction) and can propagate in the physical medium. Its propagation velocity corresponds to an acoustic wave's propagation velocity and is detected by one of the lasers. SBS imaging enables measurements with fast acquisition times free from elastic scattering background; therefore, it has been presented as a compelling alternative to conventional BS [20]. However, as SBS is based on the simultaneous application of two lasers, internal scattering may entail a critical hindering in its applicability to non-transparent samples if an initial optical clearing step is not performed. Nevertheless, its Raman homologous SRS has been successfully applied to non-cleared 1 mm thick mouse brain sections with a cellular resolution [21].

There is a growing tendency to combine Brillouin with Raman spectroscopy; therefore, a brief insight on the physical basis of the Raman effect should be provided to understand its contribution to some of the Brillouin studies that will be presented in this review. Both Brillouin and Raman scattering are based on the principle of inelastic scattering of light by phonons that are acoustic in the case of Brillouin and optical in the case of Raman. While the probing of acoustic phonons by BS provides information about the speed of propagation of lattice vibrations, which relates to the mechanical properties and density of the material, the probing of optical phonons by Raman yields information concerning the intrinsic vibrations of molecules, indicating the types of bonds that exist between them and allowing for the molecular characterization of samples. More in depth, Raman scattering is caused by intermediate electronic states that arise due to quantum vibrations specific for different molecular bond types, leading to asymmetric electronic transitions that vary in their final resting state. Raman is not a type of fluorescence emission that is characterized by energy loss in the excited electronic state but for which the resting state corresponds to the pre-excitation one [22]. Contrarily, in Raman, the electrons do not suffer energy loss in the excited state but relax into a different resting-state depending on the corresponding bond's vibrational energy, inducing a Raman frequency shift proportional to such a vibrational state [22].

2.2. Experimental Setup: Scattering Geometries

The experimental implementation of a Brillouin spectroscopy system is somewhat complicated as the photon–phonon interaction occurs within the material under study and must be described in a reference frame outside the material, namely the laboratory reference frame. This fact is very relevant and therefore the so-called scattering geometries is crucial in the BS experiment. The scattering geometries are geometrical relationships between the sample orientation, incident, and scattered light beams in the laboratory reference frame. Moreover, these scattering geometries determine the direction and magnitude of the acoustic scattering wave vector (***q***) that is fundamental for the correct interpretation of the BS experiment in general and particularly in the case of material with preferential directions as in crystals or fibers.

The most commonly used scattering geometries are 90, 90*A*, and 180 (backscattering geometry) [23]. **Figure 3**A shows the 90*A* and 180 (backscattering geometries) with the incident's geometrical relations, scattered light directions, and the acoustic wave vectors involved. As can be observed, different scattering geometries imply different orientations of the acoustic wave vector. The magnitude of the acoustic wave vector is provided by:

$$q^{90A} = \frac{2\pi\sqrt{2}}{\lambda_0}$$
$$q^{180} = \frac{n4\pi}{\lambda_0} \quad (3)$$

where λ_0 is the laser vacuum wavelength and n is the refractive index of the physical medium. The wave vector's magnitude in the 90*A* scattering geometry is independent of the refractive index of the material studied. In contrast, in the other scattering geometries, the refractive index is always present. The combination of these scattering geometries in an optically and elastically isotropic material provides the value of the corresponding refractive index:

$$n = \frac{f^{180}}{f^{90A}\sqrt{2}} \quad (4)$$

where f^{90A} and f^{180} correspond to the Brillouin frequency shift of the experiment for the 90*A* and backscattering geometries, respectively.

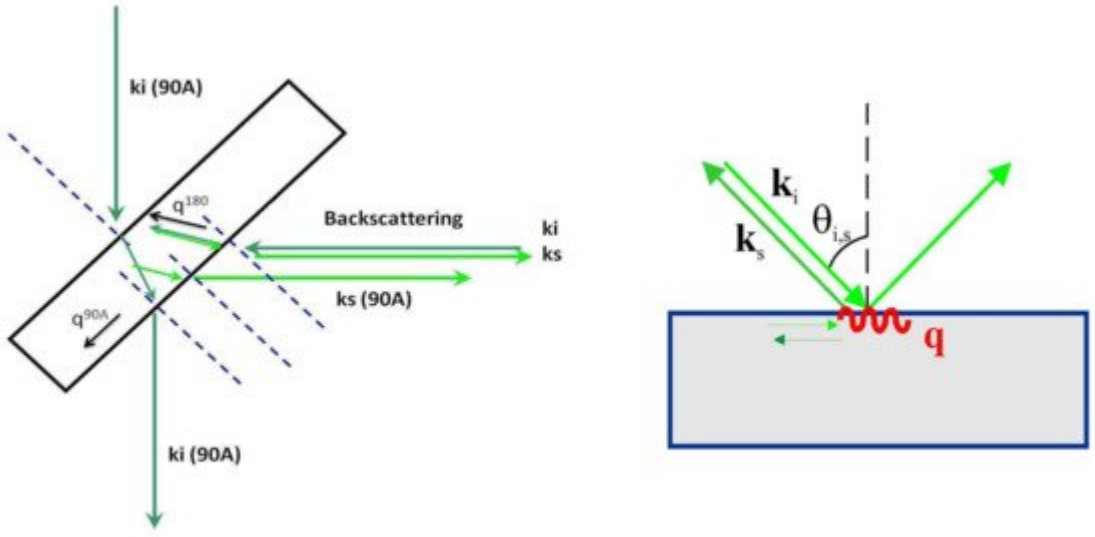

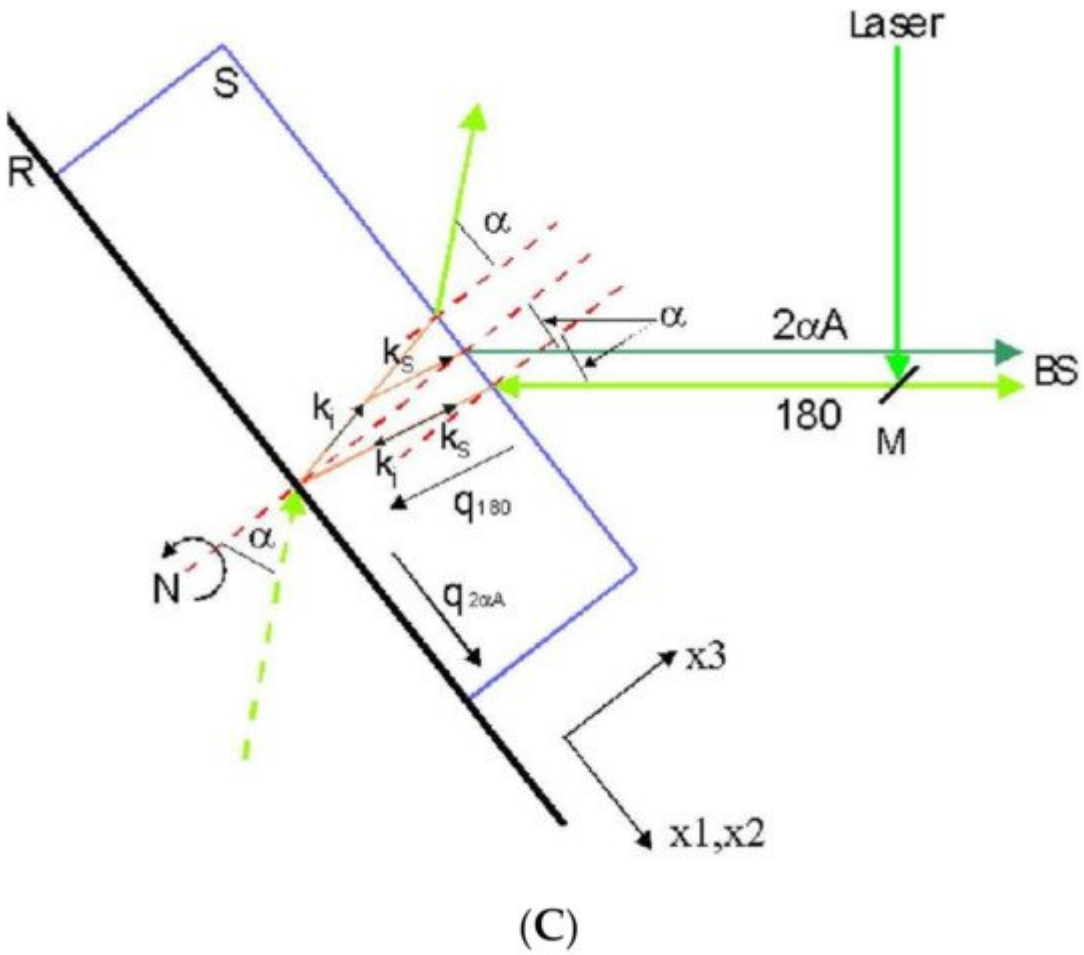

Figure 3. Representation of different scattering geometries. (**A**) 90*A* and 180 as used in solid transparent samples or liquids inside a cuvette. k_i and k_S are incident and scattered optical wave vectors, respectively. q^{90A} and q^{180} correspond to acoustic wave vectors. (**B**) Scattering geometry in an opaque material. (**C**) Scattering geometries in a film on a reflecting substrate. The reflected light beam acts as a virtual one from behind the sample. Two scattering geometries exist simultaneously: 180 and 2*αA*.

A compelling case concerns transparent film samples (thickness above 500 nm), either self-standing or resting on a reflecting substrate. As can be observed in **Figure 3**C, on the back surface of the plate, the incident light reflects and produces a supplementary light source that allows the simultaneous observation of two scattering geometries including the 180 (backscattering) and the other depending on the incident angle [24]. This second scattering geometry can be denoted as 2*αA*, similar to the 90*A* because its acoustic wave vector is independent of the refractive film index:

$$q^{2\alpha A} = \frac{4\pi \sin \alpha_i}{\lambda_0} \quad (5)$$

where α_i is the incident angle.

In opaque materials with an excellent surface optical quality of mostly metallic or semiconductor materials, the light beam is reflected on the surface and cannot penetrate the inner part of the sample. Only the projection on the material's surface of the incident and scattered light wave vectors are relevant for the scattering process. The acoustic wave vector remains on the material's surface and can only couple to its surface acoustic waves (SAW) (**Figure 3**B). In this case, the acoustic wave vector reads as follows [25]:

$$q^{SAW} = \frac{4\pi \sin \theta_i}{\lambda_0} \quad (6)$$

where θ_i is the incident angle. In magnetic materials, the magnetic field of the incident light can couple to the magnetic modes of the material (magnons) to obtain information about its magnetic properties [26].

References

1. Li, Y.; Moon, S.; Chen, J.J.; Zhu, Z.; Chen, Z. Ultrahigh-sensitive optical coherence elastography. Light Sci. Appl. 2020, 9, 58.
2. Brillouin, L. Diffusion de la lumière et des rayons X par un corps transparent homogène. Ann. Phys. 1922, 9, 88–122.
3. Brillouin, L. Influence de l'agitationthermique sur la viscosité des liquides. Propagationd'ondesélastiquesdans un milieu en mouvement. J. Phys. Radium 1922, 3, 362383.
4. Carlotti, G. Elastic Characterization of Transparent and Opaque Films, Multilayers and Acoustic Resonators by Surface Brillouin Scattering: A Review. Appl. Sci. 2018, 8, 124.
5. Gabriel, P. Light Scattering in Inhomogeneous Media; McGraw-Hill Education: New York, NY, USA, 2010.
6. Mandelstam, L.I. Light scattering by inhomogeneus media. Zh. Russ. Fiz-Khim. Ova. 1926, 58, 381.
7. Pechenkin, A. Leonid Isaakovich Mandelstam; Springer: Cham, Switzerland, 2014; ISBN 9783319005713.
8. Gross, E. überÄnderung der WellenlÄngebeiLichtzerstreuung in Kristallen. Z. Fur Phys. 1930, 63, 685.
9. Rank, D.H. Brillouin Effect in Liquids in the Prelaser Era. J. Acoust. Soc. Am. 1971, 49, 937–940.
10. Harley, R.; James, D.F.V.; Miller, A.J.; White, J.W. Phonons and the elastic moduli of collagen and muscle. Nature 1977, 267, 285–287.

11. Vaughan, J.M.; Randall, J.T. Brillouin scattering, density and elastic properties of the lens and cornea of the eye. Nature 1980, 284, 489–491.
12. Shirasaki, M. Large angular dispersion by a virtually imaged phased array and its application to a wavelength demultiplexer. Opt. Lett. 1996, 21, 366–368.
13. Koski, K.J.; Yarger, J.L. Brillouin imaging. Appl. Phys. Lett. 2005, 87, 061903.
14. Coker, Z.; Troyanova-Wood, M.; Traverso, A.J.; Yakupov, T.; Utegulov, Z.N.; Yakovlev, V.V. Assessing performance of modern Brillouin spectrometers. Opt. Express 2018, 26, 2400–2409.
15. Antonacci, G.; Beck, T.; Bilenca, A.; Czarske, J.; Elsayad, K.; Guck, J.; Kim, K.; Krug, B.; Palombo, F.; Prevedel, R.; et al. Recent progress and current opinions in Brillouin microscopy for life science applications. Biophys. Rev. 2020, 12, 615–624.
16. Kragh, H. The Lorenz-Lorentz formula: Origin and early history. Substantia 2018, 2, 7–18.
17. Carpenter, D.K. Dynamic Light Scattering with Applications to Chemistry, Biology, and Physics (Berne, Bruce J.; Pecora, Robert). J. Chem. Educ. 1977, 54, A430.
18. Berne, B.J.; Pecora, R. Dynamic Light Scattering: With Applications to Chemistry, Biology, and Physics; Dover Publications: Mineola, NY, USA, 1976.
19. Garmire, E. Stimulated Brillouin Review: Invented 50 Years Ago and Applied Today. Int. J. Opt. 2018, 2018, 2459501.
20. Remer, I.; Shaashoua, R.; Shemesh, N.; Ben-Zvi, A.; Bilenca, A. High-sensitivity and high-specificity biomechanical imaging by stimulated Brillouin scattering microscopy. Nat. Methods 2020, 17, 913–916.
21. Freudiger, C.W.; Min, W.; Saar, B.G.; Lu, S.; Holtom, G.R.; He, C.; Tsai, J.C.; Kang, J.X.; Xie, X.S. Label-Free Biomedical Imaging with High Sensitivity by Stimulated Raman Scattering Microscopy. Science 2008, 322, 1857–1861.
22. Scarponi, F.; Mattana, S.; Corezzi, S.; Caponi, S.; Comez, L.; Sassi, P.; Morresi, A.; Paolantoni, M.; Urbanelli, L.; Emiliani, C.; et al. High-Performance Versatile Setup for Simultaneous Brillouin-Raman Microspectroscopy. Phys. Rev. X 2017, 7, 031015.
23. Krüger, J.K. Optical Techniques to Characterize Polymer Systems; Bassler, H., Ed.; Elsevier: New York, NY, USA, 1989; 610p.
24. Krüger, J.K.; Embs, J.; Brierley, J.; Jiménez, R. A new Brillouin scattering technique for the investigation of acoustic and opto-acoustic properties: Application to polymers. J. Phys. D Appl. Phys. 1998, 31, 1913–1917.
25. Mutti, P.; Bottani, C.; Ghislotti, G.; Beghi, M.; Briggs, G.; Sandercock, J. Surface Brillouin Scattering—Extending Surface Wave Measurements to 20 GHz. In Advances in Acoustic

Microscopy; Springer: Boston, MA, USA, 2011.

26. Sebastian, T.; Schultheiss, K.; Obry, B.; Hillebrands, B.; Schultheiss, H. Micro-focused Brillouin light scattering: Imaging spin waves at the nanoscale. Front. Phys. 2015, 3.